SCAFFOLD OF ASYMMETRIC ORGANIC COMPOUNDS - MAGNETITE PLAQUETTES.

Q.H.S. Chan[1], M.E. Zolensky[1], J. Martinez[2], [1]ARES, NASA Johnson Space Center, Houston, TX 77058, USA. (hschan@nasa.gov), [2]Jacobs Engineering, Houston, TX 77058, USA.

Introduction: Life on Earth shows preference towards the set of organics with particular spatial configurations, this 'selectivity' is a crucial criterion for life. With only rare exceptions, life prefers the left- (L-) form over the right- (D-) form of amino acids, resulting in an L-enantiomeric excess (L_{ee}). Recent studies have shown L_{ee} for α-methyl amino acids in some chondrites [1, 2]. Since these amino acids have limited terrestrial occurrence, the origin of their stereoselectivity is nonbiological, and it seems appropriate to conclude that chiral asymmetry, the molecular characteristic that is common to all terrestrial life form, has an abiotic origin.

A possible abiotic mechanism that can produce chiral asymmetry in meteoritic amino acids is their formation with the presence of asymmetric catalysts, as mineral crystallization can produce spatially asymmetric structures [3, 4]. Magnetite is shown to be an effective catalyst for the formation of amino acids that are commonly found in chondrites [5]. Magnetite 'plaquettes' (or 'platelets'), first described by Jedwab [6], show an interesting morphology of barrel-shaped stacks of magnetite disks with an apparent dislocation-induced spiral growth that seem to be connected at the center. A recent study by Singh et al. [7] has shown that magnetites can self-assemble into helical superstructures. Such molecular asymmetry could be inherited by adsorbed organic molecules.

In order to understand the distribution of 'spiral' magnetites in different meteorite classes, as well as to investigate their apparent spiral configurations and possible correlation to molecular asymmetry, we observed polished sections of carbonaceous chondrites (CC) using scanning electron microscope (SEM) imaging. The sections were also studied by electron backscattered diffraction (EBSD) in order to reconstruct the crystal orientation along the stack of magnetite disks.

Samples and analytical methods: We analyzed polished sections of fifteen CCs spanning different classes (**CI1**: Alais, Ivuna, Orgueil; **CM1**: MET 01070,8, LAP 02422; **CM2**: Murchison, Mighei; **CO3**: ALHA77307; **CV3**: NWA 2086; **CR1**: GRO 95577; **CR2**: GRA 95229, Renazzo; **CH3**: PCA 91467; **Heated CM**: Bench Crater; **C2-ung**: Tagish Lake).

Imaging and mineral elemental compositions were obtained using the JEOL 7600F Field Emission SEM at NASA Johnson Space Center (JSC). EBSD patterns were obtained using a Zeiss SUPRA 55VP Field Emission SEM with a Bruker Quantax CrystAlign 400i EBSD system coupled with a Bruker e^-Flash EBSD detector at JSC.

Results and discussion: Magnetite plaquettes were observed in nine (Alais, Ivuna, Orgueil, LAP 02422, GRO 95577, GRA 95229, Renazzo, PCA 91467, and Bench Crater) out of fifteen CCs analyzed. Although magnetite plaquettes have been reported for Tagish Lake [8, 9], we could not find any in our sample (MG62,1). The magnetite plaquettes usually occur along fractures and sometimes were found to fill up a preexisting void. They were also observed in matrix often associated with or contained within carbonates (calcite and dolomite) and phyllosilicates, indicating an aqueous origin. We found that the abundance of magnetite plaquettes follows the sequence of CI1 > CR2 > CR1 > CM1 ≥ CH3, while we did not locate magnetite plaquettes in CM2, CO3, or CV3.

The sizes of the largest magnetite plaquettes in the CCs are 3.6 to 9.2 μm in thickness across the discs. The thickness of the individual discs range from 0.2 to 0.6 μm, and the disc spacings range from 0.1 to 0.4 nm. The number of discs in a plaquette varies from 4 to 24. These results generally agree with those reported for Orgueil by Hua and Buseck [10].

Magnetite plaquettes were sometimes found to form plate-doublets, where the spacing between the plate-doublet is significantly smaller than the spacing to the adjacent discs. This feature can be related to the crystal and magnetization orientation, such that magnetite discs with opposite orientation are drawn closer together by their magnetic polarity, so that when the magnetization align, two discs are drawn closer together, while the adjacent anti-aligned disks are positioned further away. If magnetization polarity is associated with crystal lattice, this indicates that the crystal orientation alternates across the stack of magnetite discs in a plaquette.

Spiral vs non-spiral features. One of the reasons why magnetite plaquettes have drawn decades of attention is the striking appearance of the "spiral" morphology that could have formed by dislocation-induced crystal growth [11]. The apparent spiral feature with a possible hollow core was also documented by high-resolution TEM images showing a curved twist on the terminating plates of the magnetite stack [10]. However, Sheldon and Hoover [12] argued that the magnetites were not spirals as the plaquettes were not attached to

each other, rather being separate plates held together by an exterior membrane. Therefore, a detailed description of the internal morphology of the magnetites is still lacking, which is deemed necessary in order to confirm the apparent spiral configuration.
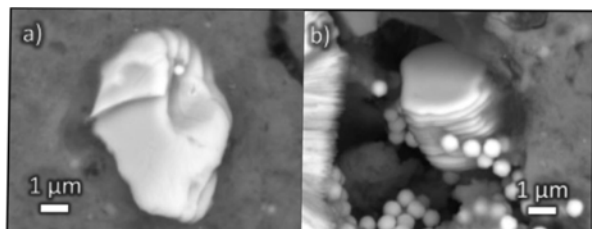

Fig 1. Magnetite plaquettes in Orgueil showing a) an "apparent" spiral and b) non-spiral features.

Some images do indeed appear to display a "spiral" appearance (Fig 1a). However, these are most plausibly laboratory-induced features caused by mechanical polishing. Several plaquettes clearly show that the surfaces of the terminating plates are smooth and are clearly devoid of a spiral feature (Fig 1b). These plates are either tilted sideway or protected by adjacent features so that the surfaces were not susceptible to the polishing effect, and thus they should retain and represent the original morphology.

EBSD analysis. We identified areas and samples of interest by SEM, then we analyzed the crystallography of magnetite plaquettes by EBSD. The observed and calculated EBSD patterns are shown in Fig 2, where the observed pattern was matched to a calculated pattern which indicates a particular crystal orientation for the analyzed spot. According to the EBSD data, the magnetite crystal orientation is fairly consistent across a single disc, changing by less than 4° across the disc. More prominent change (~40°) in crystal orientation is observed for the whole magnetite stack across several discs (Fig 3) (i.e. the crystallographic orientation changes only between disks). We have thus observed significant changes in the crystallographic orientation from top to the bottom of the stack of disks. Therefore, although individual discs are not connected and no spiral features were observed, variation in crystal orientation across the magnetite stack provides a possible rotational feature for magnetite plaquettes. The crystal orientation shifted consistently among several disks so that a rotational direction could be interpreted. The rotation direction observed was mostly but not always sinistral, with jumps of inconsistent direction that "reset" the rotation direction.
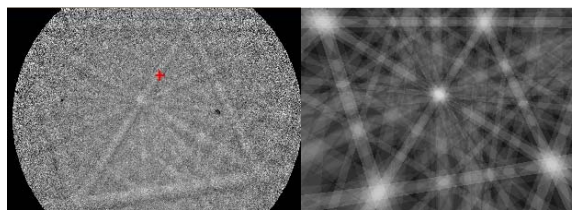

Fig 2. The observed (left) and calculated (right) EBSD patterns of an Orgueil magnetite in the cluster in Fig 3.
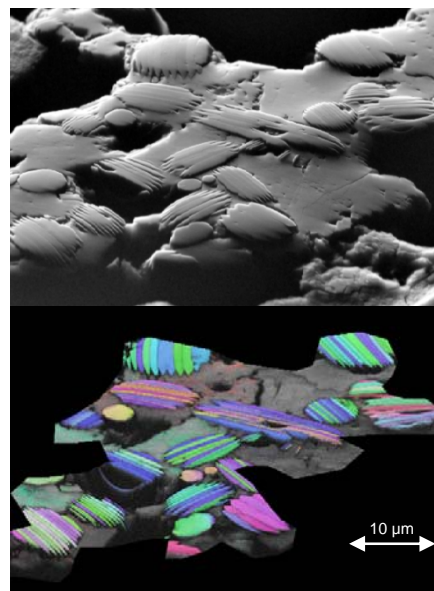

Fig 3. (Top) BSE image and (bottom) a superimposed EBSD map of a cluster of magnetite plaquettes in Orgueil.

Conclusions: We conclude that magnetite plaquettes are in reality stacks of individual discs, with crystal orientation changing significantly along the stack. Our future direction is to observe the internal morphology of magnetite plaquettes by X-ray computer tomography, and characterization of the magnetic structure of plaquettes using magnetic force microscopy, to determine whether the rotation between adjacent plates within plaquettes can influence organic chirality.

References:
[1] Glavin *et al.* (2011) *MAPS* **45**, 1948-1972. [2] Cronin and Pizzarello (1997) *Science* **275**, 951-955. [3] Pizzarello (2006) *Accounts of Chem. Res.* **39**, 231-237. [4] Pizzarello and Groy (2011) *GCA* **75**, 645-656. [5] Pizzarello (2012) *MAPS* **47**, 1291-1296. [6] Jedwab (1967) *EPSL* **2**, 440-444. [7] Singh *et al.* (2014) *Science* **345**, 1149-1153. [8] Zolensky *et al.* (2002) *MAPS* **37**, 737-761. [9] Greshake *et al.* (2005) *MAPS* **40**, 1413-1431. [10] Hua and Buseck (1998) *MAPS* **33**, A215-A220. [11] Jedwab (1971) *Icarus* **15**, 319-340. [12] Sheldon and Hoover (2012) SPIE Optical Engineering Applications, 85210N.